CHAPTER IV
RESULTS AND DISCUSSION

4.1 MMA-g-HDPE Characterization

The grafting steps of MMA monomer onto HDPE was done in Brabender batch type mixer in the presence of dicumyl peroxide (DCP) as an initiator. Besides insitu grafted product of MMA-g-HDPE, some side products were participated in the system from radical polymerization reaction e.g. poly(methyle methacrylate) (PMMA), block copolymer of MMA and HDPE, or crosslinked HDPE.

The efficiency of grafting was determined by comparing the carbonyl group absorbance of grafted monomer to the methyl group absorbance of HDPE. The percentage of grafting (PG) and the total reaction efficiency (TE) were 2 parameters which were used to define the extent of reaction.

PG = (Weight of MMA grafted on HDPE/ Initial weight of MMA) x100

TE = (Weight of MMA converted/ Initial weight of MMA) x100

4.1.1 Calculation of Percent Grafting and Total Reaction Efficiency

From FT-IR spectra, the integral area of carbonyl (C=O) peak (1730 cm^{-1}) and CH bending peak (1368 cm^{-1}) were obtained. The integral ratio was calculatated by following equation.

Integral ratio = Integral area of C=O peak/integral area of CH bending peak

The integral area of C=O peak, integral area of CH peak, and integral ratio of HDPE modified with 10 % wt of MMA, DCP:MMA = 1:40 equivalent mole were shown as followed.

	Crude	Purified
Integral area of C=O peak	4.2024	2.0465
Integral area of CH bending peak	0.7886	0.9521
Integral ratio	5.329	2.1515

Percent weight of MMA in the sample was calculated from the calibration curve (Figure 3.1)

$$\text{Percent weight of MMA in the sample} = \frac{\text{Integral ratio}}{0.9387}$$

Therefore :

$$\text{Percent weight of MMA in purified sample} = \frac{2.1515}{0.9387} = 2.292\ \%$$

$$\text{Percent weight of MMA in crude sample} = \frac{5.3290}{0.9387} = 5.677\ \%$$

Percentage of grafting and total reaction efficiency were calculated by percent weight of MMA used in purified sample and crude sample which are the weight of MMA grafted on HDPE and weight of MMA converted respectively.

Thus :

$$PG = (\text{Weight of MMA grafted on HDPE/ Initial weight of MMA}) \times 100$$

$$= \frac{2.292 \times 100}{10} = 22.92\ \%$$

TE = (Weight of MMA converted/ Initial weight of MMA) x100

$$= \frac{5.677 \times 100}{10} = 56.77\ \%$$

Content of MMA-g-HDPE of 22.92% wt as the compatibilizer is considered to be appropriate amount when converted to the % total weight.

Initial weight	HDPE	=	90	g
	MMA	=	10	g
	Total	=	100	g

Therefore: Crude sample 100 g contains MMA-g-HDPE 2.292 g.

4.1.2 Gel Content Determination

After the crude samples of MMA-g-HDPE (1g) were refluxed in 100 ml of o-dichlorobenzene for 24 hr to determine the insoluble portion (gel) in the sample. It was found that gel content was 0.2% by weight at the 10% weight initial MMA concentration on HDPE and DCP:MMA = 1:40. Thus it is noted that one-step blending samples contain both 0.2% wt gel and about 2.4% wt PMMA or MMA residue while two-step blending contains only gel part.

4.2 Effect of Fiber Loading on the Mechanical Properties of the Blends

4.2.1 Tensile Modulus

Tensile modulus increased with increasing fiber loading due to the presence of fiber with high modulus, so that the blends were stiffer. Comparing between 2 techniques, reactive blending gave higher modulus. This reason can be explained by the different processing conditions. First, in two-step blending, silk was subjected to the heat for a long time (25min) which caused thermal degradation of silk during processing. Moreover, it was

extruded with a high shear rate (80 rpm) leading to breakage of fiber and lowering properties compared to those of reactive blending which took 10 min of blending at 160°C.

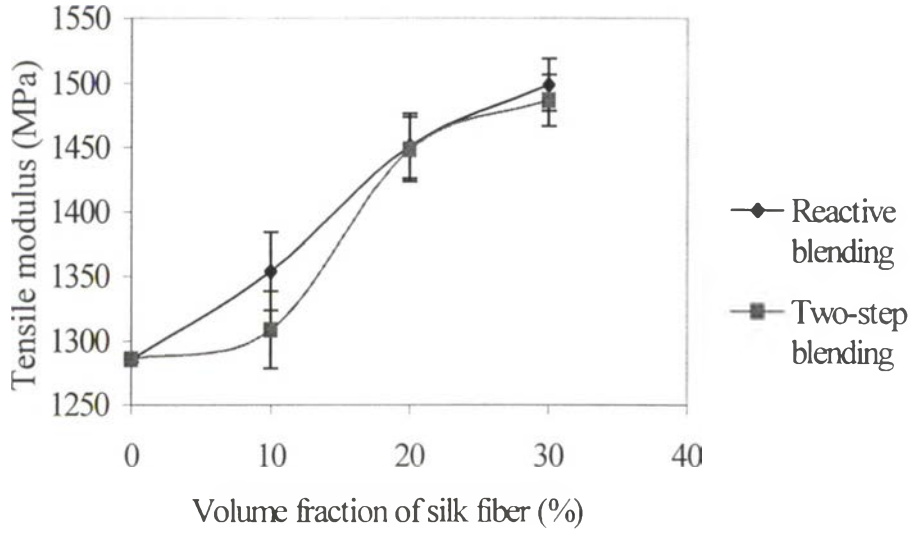

Figure 4.1 Effect of fiber loading on tensile modulus of MMA-g-HDPE/silk blends with 10, 20, 30 % SF.

4.2.2 Tensile Yield Strength

Effect of fiber loading on the tensile strength was shown in Figure 4.2. Tensile strength increased continuously with increasing fiber except at low fiber loading in which appeared to be a decrease. At low concentration of fiber, instead of being a reinforcing fiber, silk acted as the defect. Then high strain was localized in the matrix causing the bond between fiber and matrix broken. This led to the matrix diluted by non-reinforcing and debonded fiber called "Dilusion Effect" (Akhtar, S., 1986). After the fiber concentration increased, the matrix was restrained by high volume of fiber, and the stress is more evenly distributed; thus higher tensile strength was obtained.

Comparing between two techniques, reactive blending still gave higher value of tensile strength than that of two-step blending for the same reasons mentioned above.

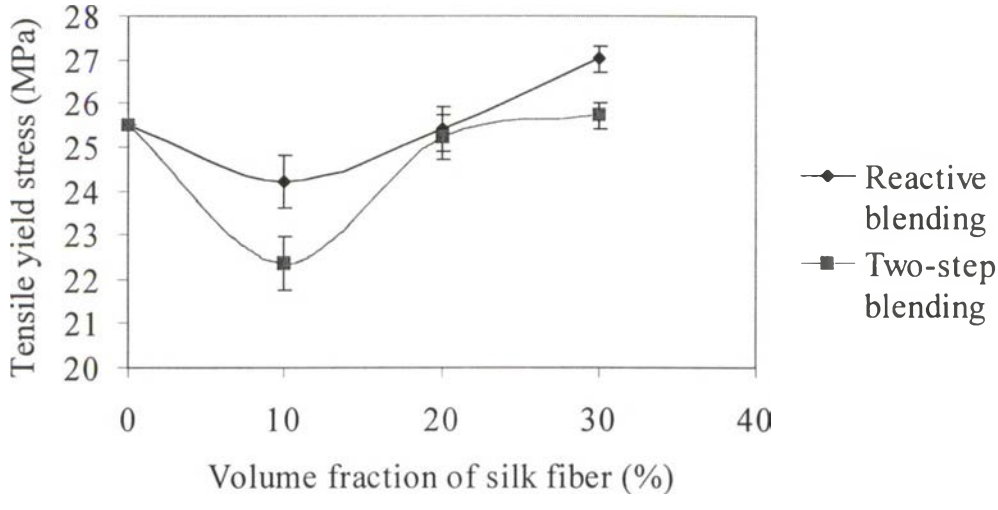

Figure 4.2 Effect of fiber loading on tensile yield strength of MMA-g-HDPE/silk blends with 10, 20, 30 % SF.

4.2.3 Flexural Modulus

The flexural modulus of the blends showed the same trend as tensile modulus that increased at higher fiber loading. However, at low fiber loading, flexural modulus decreased by the dilution effect (Akhtar, S., 1986). Reactive blending still gave higher value than those of two-step blending.

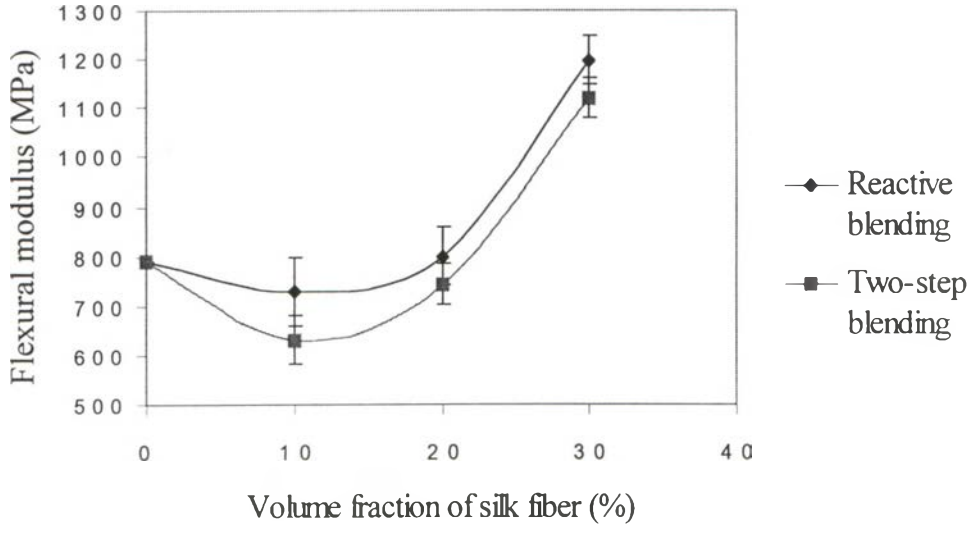

Figure 4.3 Effect of fiber loading on flexural modulus of MMA-g-HDPE/silk blends with 10, 20, 30 % SF.

4.2.4 Flexural Strength

At the low concentration of fiber, the flexural strength trended to decrease rapidly as shown in Figure 4.4 However, at high concentration of fiber, it showed the significant trends of increasing resulted from that fiber made the composite stiffer, then higher applying force was used to bend the composite.

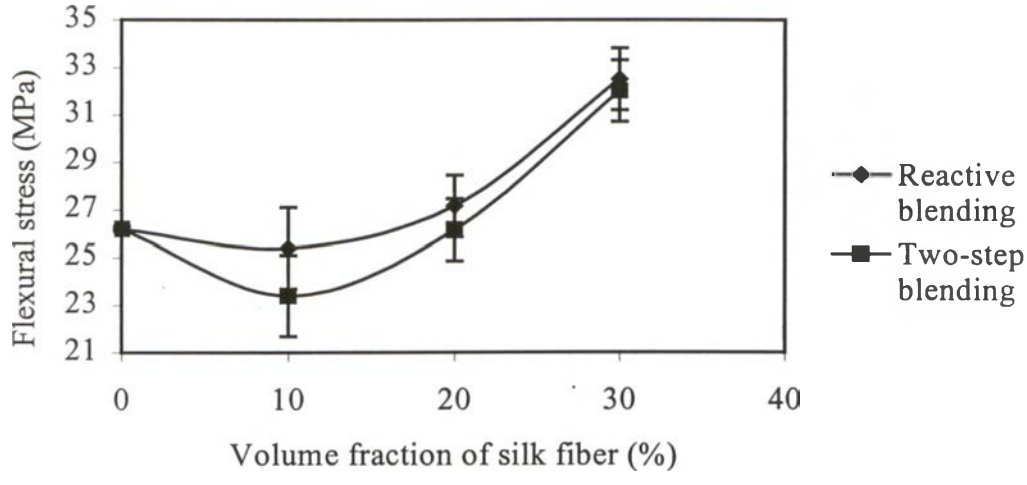

Figure 4.4 Effect of fiber loading on flexural strength of MMA-g-HDPE/silk blends with 10, 20, 30 % SF.

4.2.5 Impact Resistance

However, for impact testing, it was found that the impact resistance of the final blends decreased rapidly for both techniques as shown in Figure 4.5. This was explained by the presence of gel or crosslinking of HDPE occurring in the blending step of grafting mechanism which was 0.2% gel content that led to very low impact resistance. Nevertheless, at high fiber loading, impact strength moderately restored due to the presence of fiber network in the composite that obstructs the crack growth of impact force.

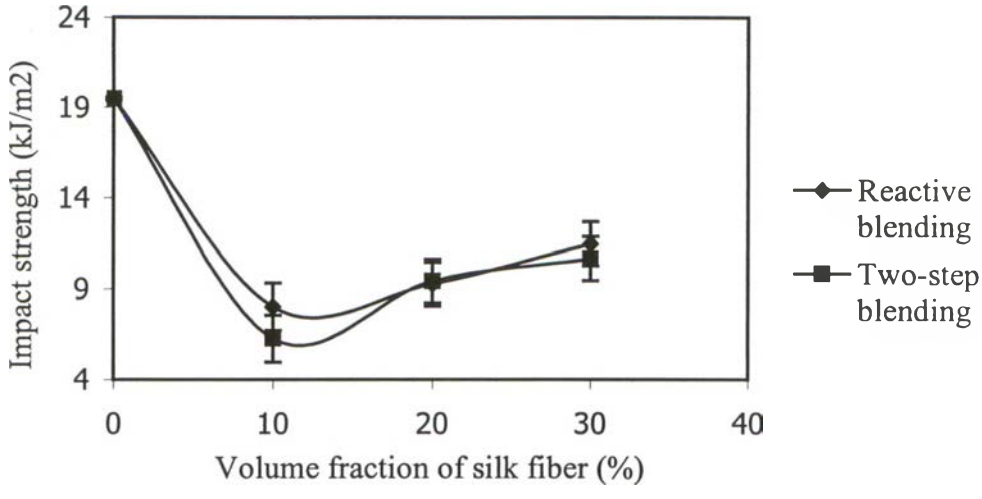

Figure 4.5 Effect of fiber loading on impact resistance of MMA-g-HDPE/ silk blends with 10, 20, 30 % SF.

4.3 Specific Interactions in MMA-g-HDPE/Silk Blends

Improving miscibility of HDPE and silk and then enhancing mechanical properties of the blends can be explained by the specific interactions between MMA-g-HDPE and silk via hydrogen bonds. According to Figure 4.6, MMA-g-HDPE shows the absorption bands as the pure component of both MMA and HDPE. There were the peaks of C=O at 1730-1740 cm^{-1} and C-O at 1100-1200 cm^{-1} from the presence of MMA grafted on the product (Maji *et al.*, 1996). However, when silk was added, there were new absorbance bands range of 3000-4000 cm^{-1} and 1700-1600 cm^{-1} due to the amide and carbonyl group of silk as shown in Figure 4.7. Moreover, the bands became broader, and the intensity increased with increasing fiber loading due to the effect of specific interaction; hydrogen bonds; at the interface of the components.

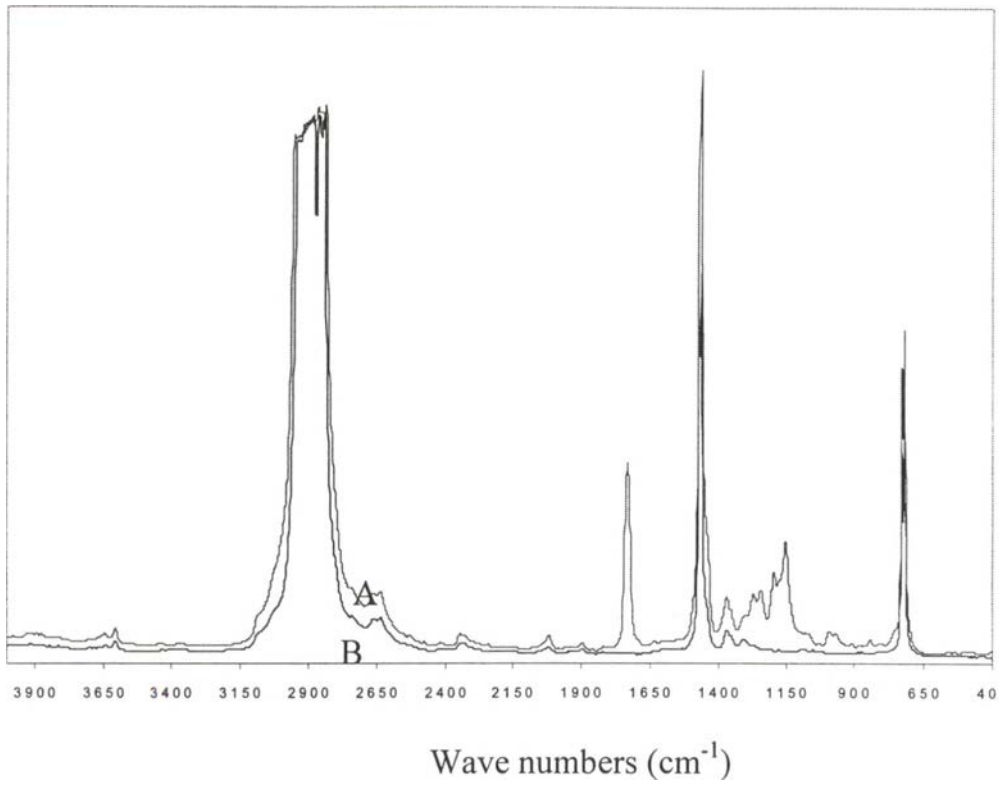

Figure 4.6 FT-IR Spectra of : (A) MMA-g-HDPE, (B) pure HDPE.

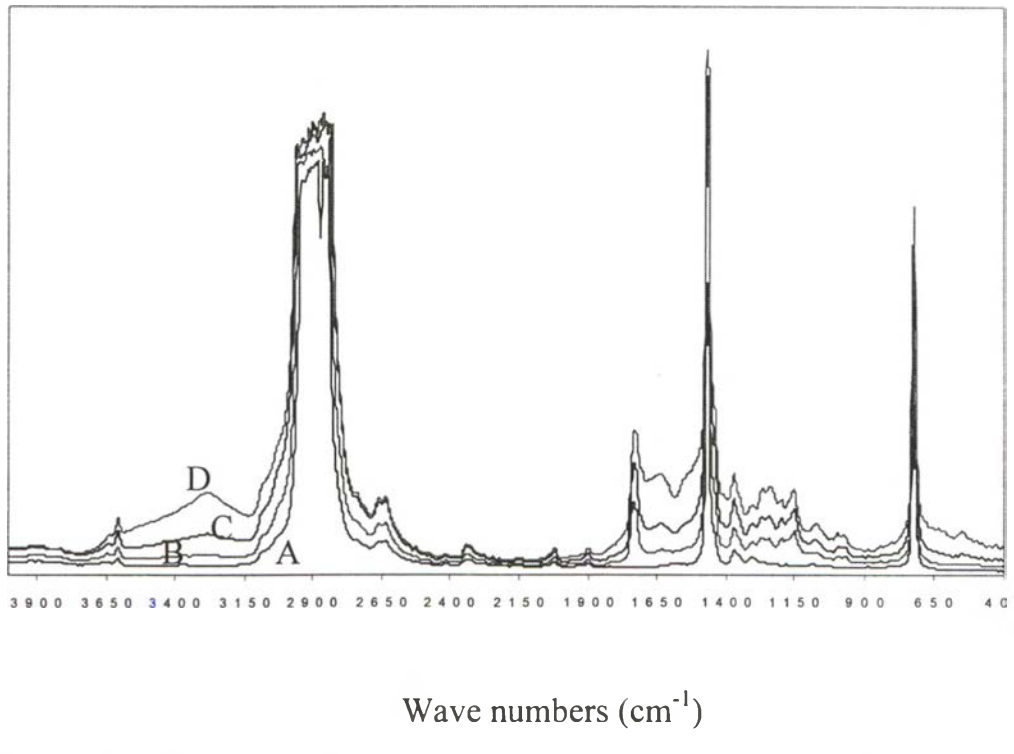

Figure 4.7 FT-IR Spectra of : MMA-g-HDPE/SF blends containing (A) 0%, (B) 10%, (C) 20%, (D) 30% SF.

Figure 4.8 showed interaction of C=O band in MMA-g-HDPE in the presence of silk. It was found that C=O band of MMA-g-HDPE at 1730 cm^{-1} became broader and the peak at 1705 cm^{-1} became apparent with increasing silk contents. This reflected the wide spread distribution of hydrogen bonds occurring between some parts of silk functional groups and MMA-g-HDPE functional groups in the distance and geometry all over the component (Sun *et al.*, 1997)

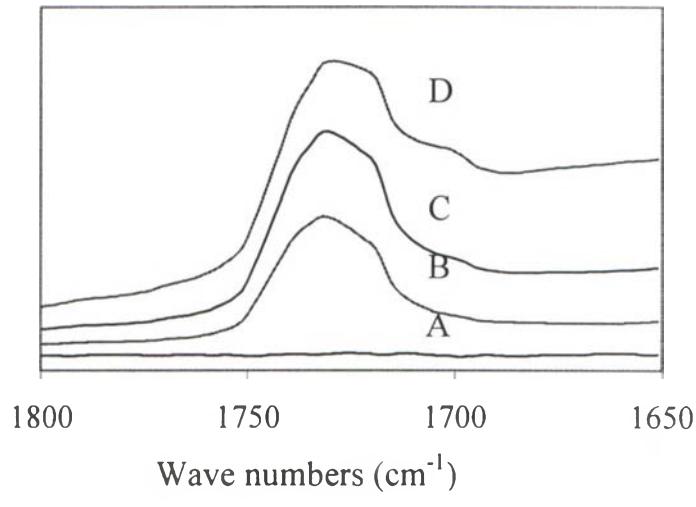

Figure 4.8 FT-IR Spectra in the range of : 1650-1800 cm^{-1} of MMA-g-HDPE/SF blends containing (A) 0, (B) 10, (C) 20, (D) 30 % SF.

Another interesting effect was the peak of C-O of MMA-g-HDPE at 1130 cm^{-1}. It became broader and also shifted to the higher frequency 1130 cm^{-1} as shown in Figure 4.9. This can be explained by the presence of silk in the blends. At high silk content, there were possible amide groups to form H-bond with the matrix, and these amide groups had lone pair electrons which delocalized from N position to C=O position. Then H-bonds were interupted by the repulsive force between C=O of silk and C=O of MMA-g-HDPE. The peak is then shifted to the higher frequency.

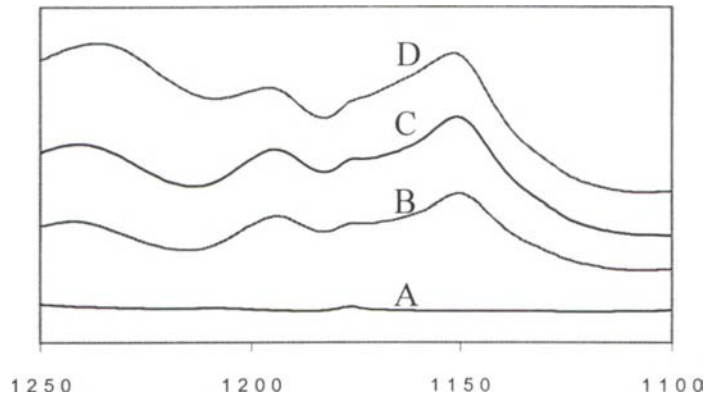

Figure 4.9 FT-IR Spectra in the range of : 1100-1250 cm^{-1} of MMA-g-HDPE/SF blends containing (A) 0, (B) 10, (C) 20, (D) 30 % SF.

Figure 4.10 showed the new absorbance band centered from 3100-3500 cm^{-1} due to the presence of silk. This was attributed to the frequency of amine and hydroxyl groups of silk, and this band was broad which indicated intramolecular H-bond within silk itself (Sun *et* al., 1997). However, it was observed at about 3750-3850 cm^{-1} which appeared to be the H-bond between OH of silk and C=O of MMA-g-HDPE. However, the intensity was low and the band was not outstanding compared to those of 3100-3500 cm^{-1} peaks. Therefore, intermolecular H-bond of hydroxyl and C=O of MMA-g-HDPE was weaker than intramolecular H-bond in silk structure as a result of competitive carbonyl groups in silk and MMA to amine and hydroxyl groups of silk fibers.

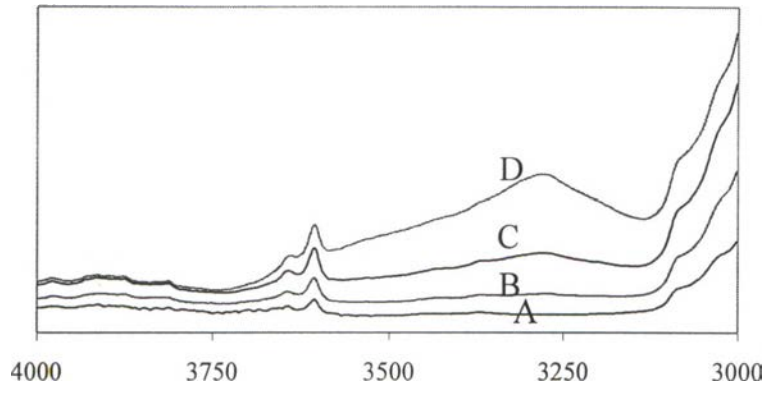

Figure 4.10 FT-IR Spectra in the range of : 3000-4000 cm^{-1} of MMA-g-HDPE/SF blends containing (A) 0, (B) 10, (C) 20, (D) 30 % SF.

Specific Interactions in MMA-g-HDPE/Silk Blends

1. Intramolecular interaction in silk by amino acid.
2. Simple H-bond between MMA and silk.
3. Possible H-bond between C-O and silk.
   - 3.1 Silk backbone.
   - 3.2 Silk side group.
4. Simple H-bond between MMA and silk side group.

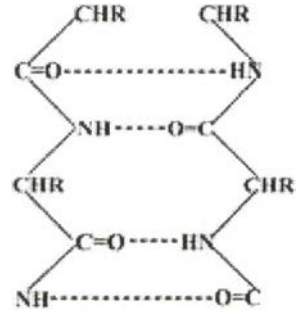

Figure 4.11 Intramolecular interactions in silk structure by amino acid.

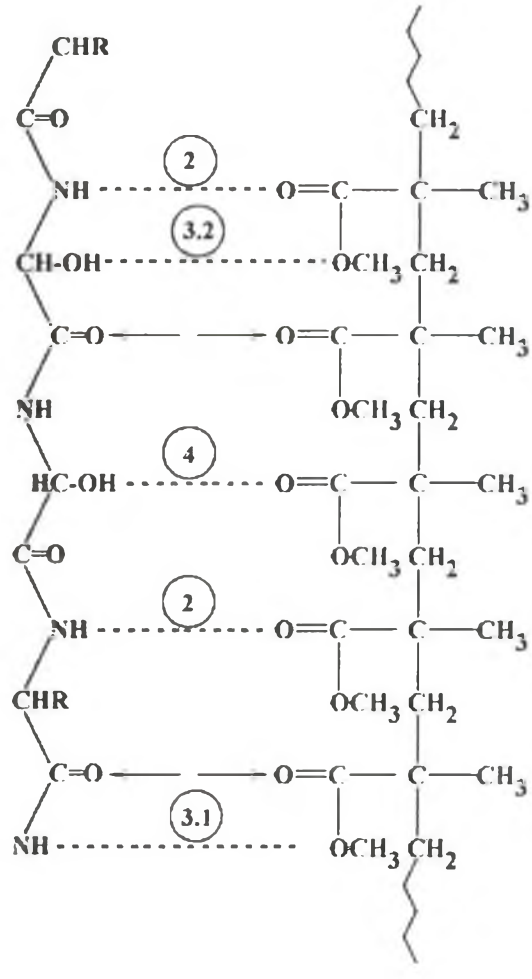

Figure 4.12 Intermolecular interactions between MMA-g-HDPE and silk.

4.4 Thermal Properties of MMA-g-HDPE/Silk Blends

The degradation temperature of the composite from one-step reactive blending was shifted to the higher temperature in the range between those of the pure components of both HDPE and silk as shown in Figure 4.11. Td of silk was about 380°C and Td of pure HDPE was 475°C (Tsukada *et al.*, 1993). From the view point of silk, Td of the composite was improved to the higher temperature from 380 to 440, 465, and 469°C with increasing fiber loading. This was evident that silk structure had stronger intermolecular

interaction, as described in the previous part, indicating more thermal stability of the blends. However, silk has very complex structure and various types of amino acids, then it cannot be determined the significant functional groups that change in this stage.

From DSC analysis shown in Table 4.1, it was found that Tg and Tm of the composite did not show the significant changing from the pure component. However, Tc was shifted to the higher temperature with increasing fiber loading. This was explained that silk acted as the nuclei of the crystallization of PE leading to faster nucleation step, so that higher Tc was achieved.

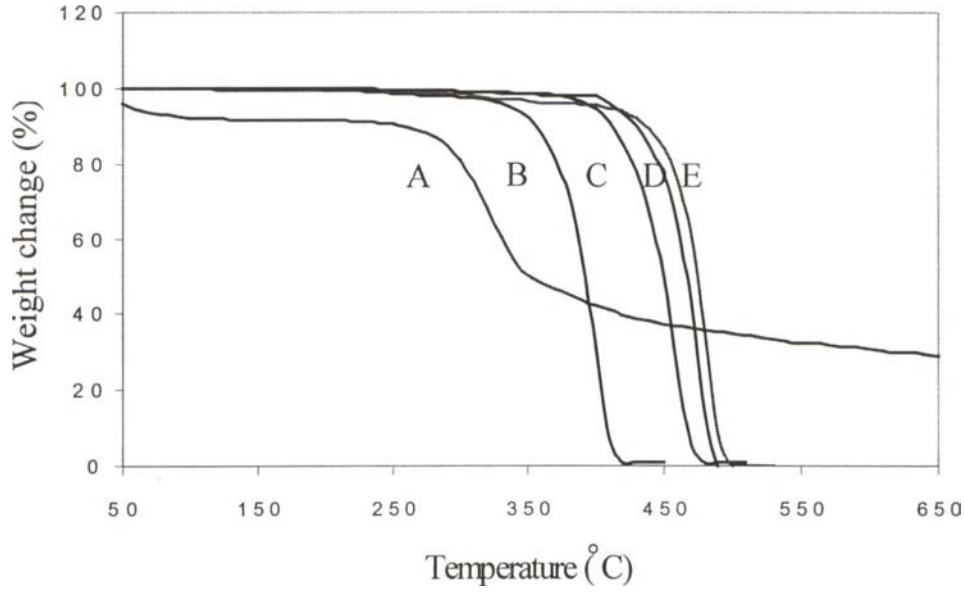

Figure 4.13 Thermal degradation temperature of MMA-g-HDPE/silk blends (A) Pure silk, (B) 10%, (C) 20%, (D) 30% SF, (E) Pure HDPE by TGA.

Table 4.1 Thermal properties of MMA-g-HDPE/silk blends by DSC.

Components	Tg(°C)	Tc(°C)	Tm(°C)
HDPE	- 115	112.8	131.9
Silk	179	-	-
PMMA	85 - 105	-	-
MMA-g-HDPE/ 10% silk fiber	- 116	113.9	131.5
MMA-g-HDPE/ 20% silk fiber	- 114.5	114.5	131.3
MMA-g-HDPE/ 30% silk fiber	- 115	116.0	132.0

4.5 MMA-g-HDPE Morphological Characterization

The morphology of the impact fracture surfaces of silk fiber filled HDPE with different mixing method was investigated by scanning electron microscope (SEM). SEM micrographs of untreated blends of HDPE with 10%, 20%, and 30% silk contents by twin screw extruder were shown in Figure 4.14 A, B, and C respectively. According to the immiscibility between silk and HDPE, it was found that 2-phases of silk and HDPE were completely separated from each other (big hole or separation between silk fiber and HDPE). Moreover, the more percent of fiber loading, the more voids and loose fiber ends sticking out of HDPE surfaces which resulted in lowering mechanical properties with increasing fiber loading of untreated HDPE/silk blends.

Figure 4.15 A, B, and C showed the impact fracture surfaces of MMA-g-HDPE/10, 20, and 30% silk blends by two-step blending method (twin screw extruder). It was found that there were not only some loose fiber ends sticking out from the surfaces but also some fibers embedded tranversly across the surface according to the random distribution of fibers. Furthermore, There were less voids occurring on the matrix surfaces compared to untreated blends. Some of fibers were still attached to the matrix, and the gaps between fiber surfaces and matrix happened to be less compared to untreated blends. The fracture behavior of the blends was in the brittle like in the presence of MMA while it was in ductile like in untreated blends due to less adhesion between fiber and matrix. It was seen that some fibers break into small short fibers which can contribute to the reducing in reinforcement effect.

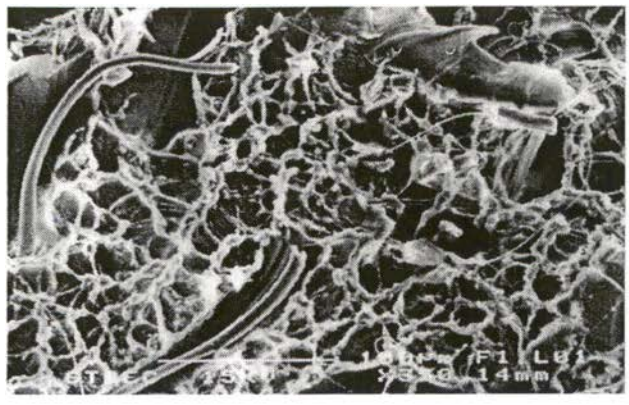

(A)

(B)

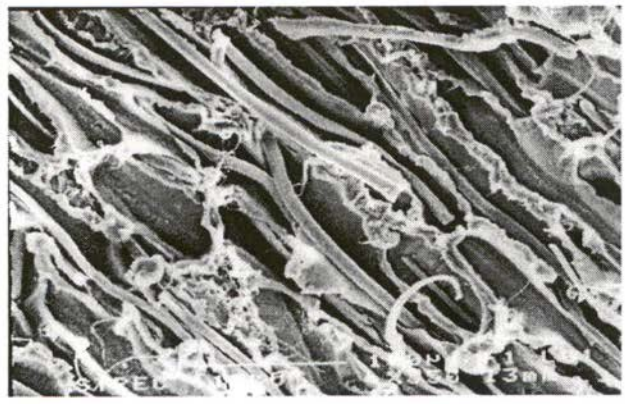

(C)

Figure 4.14 SEM micrographs of the impact fracture surface of untreated blend of HDPE/silk by screw extruder method with (A) 10%, (B) 20%, (C) 30% silk contents.

(A)

(B)

(C)

Figure 4.15 SEM micrographs of the impact fracture surface of MMA-g-HDPE/ silk by two-step blending method with (A) 10%, (B) 20%, (C) 30% silk contents.

The SEM micrographs of one-step reactive blending of MMA-g-HDPE / 10, 20, 30 % silk were shown in Figure 4.16 A, B, and C respectively. The morphology of these blends showed better homogeneous matrix than the two-step blending. However, there were less fiber ends sticking out of the surfaces. The fibers embedded smoothly in the matrix, and the gap between fibers and HDPE were hardly seen. This result can be explained by the higher bonding of fiber with HDPE by MMA grafting procedure which resulted in the fracture of fiber at the crack plane with a few fiber pullout. It was important that in fiber filled composites, a significant phenomena of the energy absorption during impact took place through fiber pullout process. In the MMA-g-HDPE/ silk blends, less fiber pullout occurred due to the higher interfacial bonding between fiber and matrix phases.

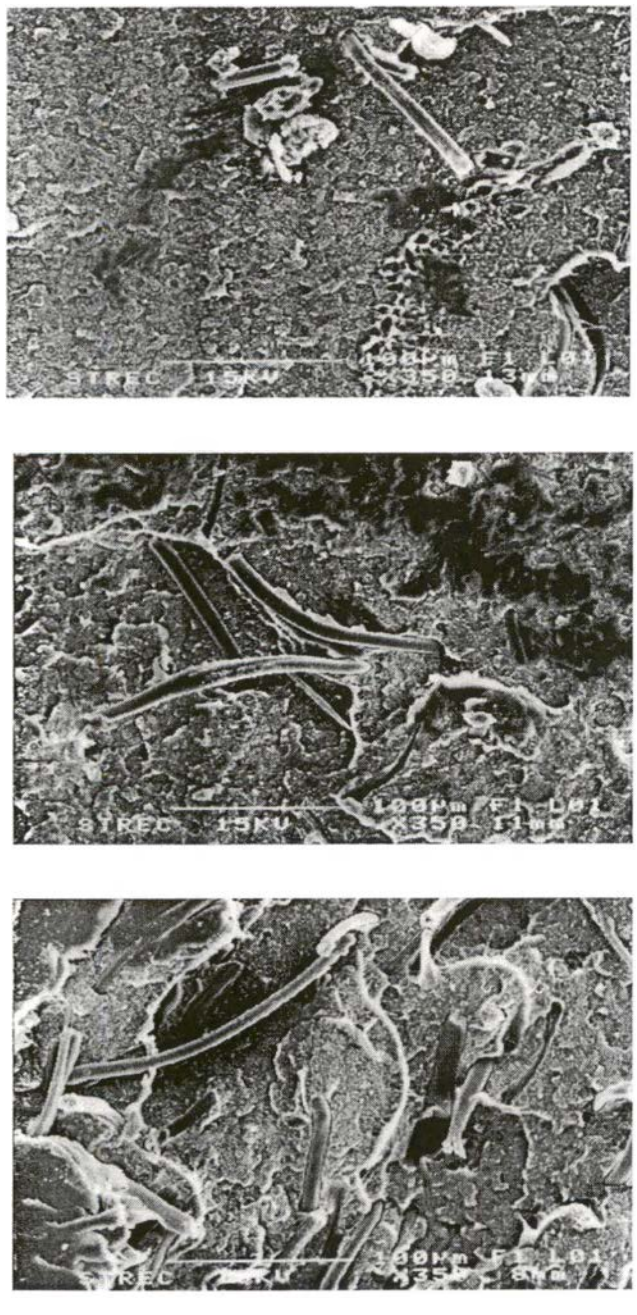

(A)

(B)

(C)

Figure 4.16 SEM micrographs of the impact fracture surface of MMA-g-HDPE/ silk by one-step reactive blending method with (A) 10%, (B) 20%, (C) 30% silk contents.

4.6 Effect of Chemical Treatment on Interfacial Adhesion

According to the immiscibility between HDPE matrix and silk fiber, the interfacial modification should be done to achieve the required properties of the blends. The interface is the area with some molecular layers whose properties are between those of the matrix and fiber phases because of peculiar restrictions on molecular motion in this area (Geethamma, *et al.*, 1998). The interfacial adhesion can be determined by the coating of matrix molecules onto fiber or the anchoring of the fiber into matrix itself not only by chemical reaction but also by mechanical process. In this work, the interfacial adhesion was improved by the addition of functionalized polymer components, methyl methacrylate monomer (MMA) onto HDPE matrix to establish carbonyl group which can interact with silk's carbonyl or amide group. The presence of the third component, MMA-g-HDPE, in the HDPE/silk blends has improved the interfacial adhesion not only via H-bond by carbonyl group but also via the formation of an interlayer between matrix and fiber. The interlayer was produced by a coating of polymer matrix molecules onto surface of silk fiber.

Figure 4.17 and 4.18 showed the SEM micrographs of the fiber surface pulled out from the cracking plane of impact specimens in MMA-g-HDPE/silk blends (with 20 % fiber contents) in one-step reactive blending and two-step blending respectively. It was found that the surfaces of silk in both methods were coated by the matrix. Especially in one-step reactive blending, the matrix was coated and formed interlayer all over the length of silk fiber while in two-step blending the fiber surface carried polymer matrix particles spreading all over the surface.

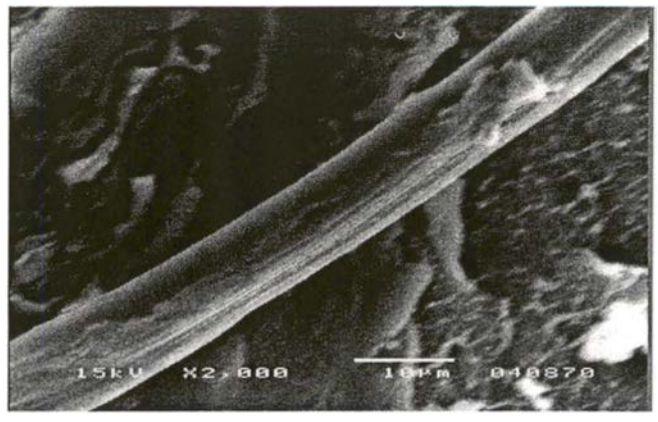

Figure 4.17 SEM micrograph of fiber surface from impact cracking plane of MMA-g-HDPE/silk (20 %) blends by one-step reactive blending method.

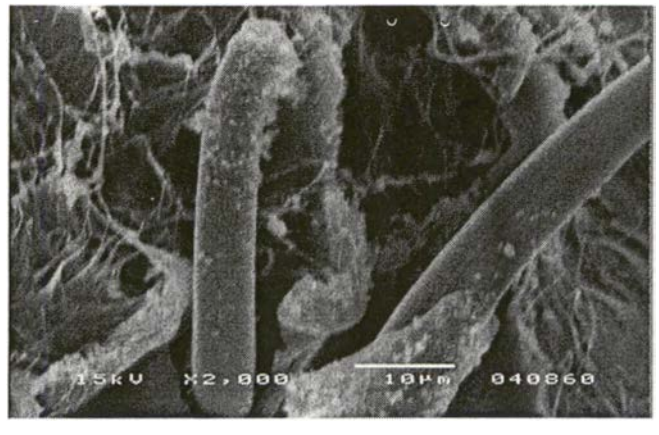

Figure 4.18 SEM micrograph of fiber surface from impact cracking plane of MMA-g-HDPE/silk (20 %) blends by two-step blending method.

The coating of polymer molecules or the polymer matrix particles on the fiber surfaces acted as the interlayer between 2 phases of the blends leading to more homogenity of the blends which can be easily seen in Figure 4.16 B (one-step reactive blending) and Figure 4.15 B (two-step blending) comparing to untreated blends in Figure 4.14 B. This contention was supported by the experimental results of an increase in tensile strength of MMA-g-HDPE/silk blends with 30% fiber contents in one-step reactive blending (27.00 MPa) and in two-step blending (25.729 MPa) comparing to untreated blends at the same fiber contents (22.842 MPa). Moreover, one-step

reactive blending showed more homogenity on the morphology comparing to two-step blending which showed more crosslinking of HDPE.

Figure 4.19 A, B, C showed silk fiber surfaces of one-step reactive blending of MMA-g-HDPE/silk blends in more details. It was found that the matrix was coated all over the fiber surface. It was hardly to be seen the fiber breakage or bending and kinking of fiber. Moreover, there was no splitting of a fiber into single filaments (of smaller diameter) because most of the fiber surface area was coated all over by the matrix. Then each fiber had low possibility to split into filaments. There was an evident for strong interfacial adhesion that part of deformed matrix was attached to the fiber.

Figure 4.20 A, B, and C showed silk fiber surfaces of two-step blending of MMA-g-HDPE/silk blends. There were more fiber breakage or bending and kinking of fiber in two-step blending comparing to one-step reactive blending. This might be the result from the processing conditions with high temperature, high mixing speed, and long mixing time leading to fiber degradation. Furthermore, in two-step blending just only some parts of fiber surfaces carried little particles of polymer matrix. Therefore, some other parts of the fiber surface were still free without any protection leading to more possibility of fiber breakage then lowering mechanical properties.

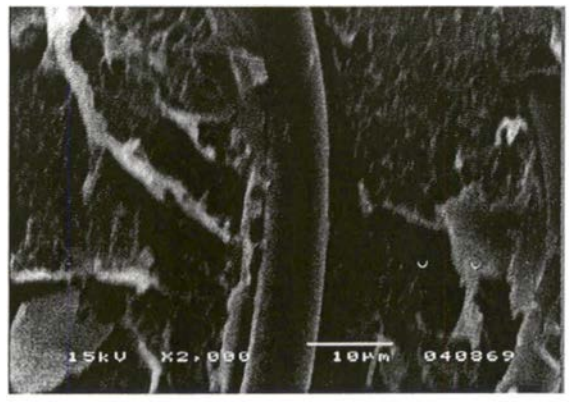

(A)

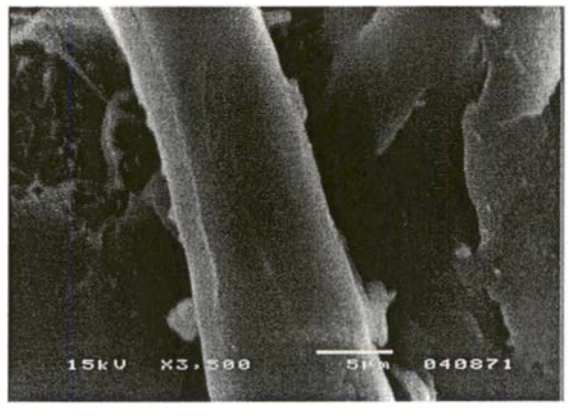

(B)

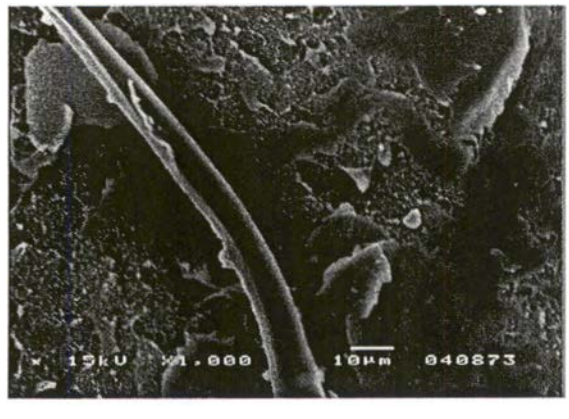

(C)

Figure 4.19 SEM micrographs of fiber surface from impact cracking plane of MMA-g-HDPE/silk (20 %) blends by one-step reactive blending method, (A) 2000 X, (B) 3500 X, (C) 1000 X.

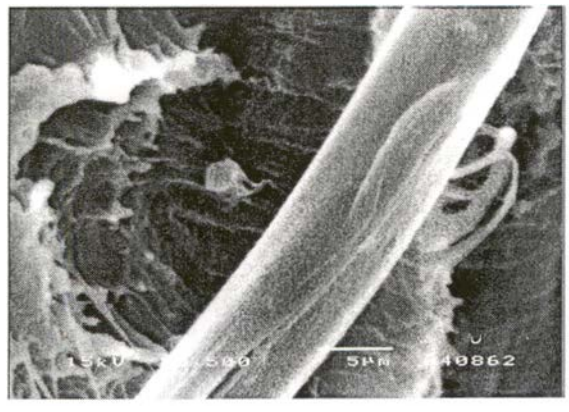

(A)

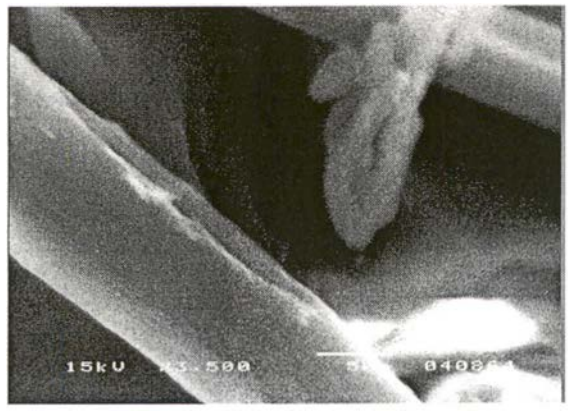

(B)

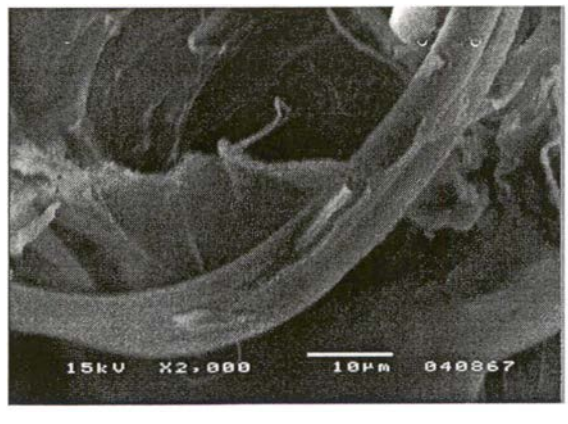

(C)

Figure 4.20 SEM micrographs of fiber surface from impact cracking plane of MMA-g-HDPE/silk (20 %) blends by two-step blending method, (A) 3500 X, (B) 3500 X, (C) 2000 X.